Proceedings of the
Annual Stability Conference
Structural Stability Research Council
Atlanta, Georgia, April 21-24, 2020

The effect of transverse stiffeners on the torsional buckling of thin-walled columns

Trung Hoang[1], Sándor Ádány[2].

Abstract
In this paper the effect of transverse stiffeners on the torsional buckling of thin-walled members is discussed. Though the torsional behavior of thin-walled members is a classic topic of structural engineering university courses, there is no comprehensive understanding on how the transverse stiffeners modify the behavior. In this paper an analytical approach is presented, which, at least in simpler cases, leads to closed-formed solution for the critical force. The analytical solutions are compared to shell finite element solutions, using a general purpose finite element software as well as the specific constrained finite element method, which has just recently been extended to handle members with transverse plate elements. The results illustrate the applicability and also the limitations of the various methods. The analytical solutions are helpful in understanding the effect of transverse stiffeners on the torsional behavior. Moreover, the results suggest that the transverse stiffeners have beneficial, and sometimes considerable effect on the critical load to pure torsional buckling of columns, which effect could be considered also in the design.

1. Introduction
Buckling is essential in analyzing thin-walled members. There are various buckling types, depending on the loading of the member and depending on the displacements involved in the buckling. Even if we limit our investigations to buckling types characterized by practically rigid cross-sections, various buckling types exist. In the case of columns flexural, pure torsional and flexural-torsional buckling types are usually distinguished; in the case of beams the global buckling is termed lateral-torsional buckling. In most of these buckling types torsion plays important role. Though from practical aspect the pure torsional buckling is rarely governing, this is the simplest form of buckling with torsion, therefore the proper understanding of pure torsional buckling can help in solving other, more frequent buckling problems, too.

Torsional behavior of thin-walled members is complicated, characterized by both Saint-Venant torsion (which induces shear stresses only) and warping (which induces axial and shear stresses). The classic description of the problem is presented in textbooks, e.g. in Vlasov (1961). Though the underlying differential equation (D.E.) is known, the exact analytical solution is challenging even for the simplest cases. There is limited number of research on pure torsional buckling of

[1] PhD student, Budapest University of Technology and Economics, <hoang.trung@epito.bme.hu>
[2] Associate Professor, Budapest University of Technology and Economics, <sadany@epito.bme.hu>

columns, though some specific problems are addressed recently, e.g. in Chroscielewski et al (2006), Rao and Rao (2017), Taras and Greiner (2008). In this paper the investigation of pure torsional buckling of columns, with a special focus on the effect of transverse plate elements, is reported.

In thin-walled members in many cases transverse plate elements are applied. Such transverse plate element may appear as an end-plate, a gusset plate, or a transverse stiffener. Though stiffeners, end-plates and gusset plates have different roles and might have different shapes, etc., they have very similar mechanical effect on the torsional behavior of members. Thus, the term "transverse stiffener" will mostly be used in this paper, but in a general meaning.

According to the authors best knowledge analytical solution for torsional buckling of thin-walled columns/beams with directly considering transverse stiffeners or end-plates is not yet reported. Analytical considerations hardly appear in the literature, which is especially true for pure torsional buckling. In Fujii and Ohmura (1985) a similar question is partially discussed, but no solution is presented. Therefore, in this paper first analytical solution for the critical load to pure torsional buckling of thin-walled columns with transverse elements is briefly reported. Then numerical investigations are presented: analytical results are compared to those from shell finite element solutions. The finite element results are produced by using the commercial finite element software Ansys (2019), and also by using the special constrained finite element method (cFEM), as in Ádány (2018) and Ádány et al. (2018), which has just recently been extended to members with transverse plate element, see Trung and Adany (2019). The examples justify the validity of the provided analytical solutions, as well as give a hint on their application limits.

2. Analytical solution: I-section members with rectangular stiffeners

2.1 Overview

The analytical solution for pure torsional buckling is derived here for a doubly-symmetrical I-section column supplemented by rectangular plates. The member itself is modelled as a one-dimensional element with cross-sections perpendicular to the member axis, i.e., a beam-model is adopted. The cross-sections are assumed to be rigid, hence the displacement of the member are given by the displacement function of the member axis. Classic beam theory is assumed, that is for the torsional behavior Vlasov's theory is applied (which can be regarded as the extension of the classic Euler-Bernoulli beam theory). The material is linearly elastic, isotropic. The stiffeners are kept symmetric with respect to the web position and also perpendicular to the member axis. The member is assumed to have n_{st} transverse plates, the position of each is given by $x_{st,i}$ ($i = 1, \ldots, n_{st,} 0 \leq x_{st,i} \leq L$); L is the length of the member. As Fig. 1a) illustrates, the depth and width of the member cross-section is h and b, respectively, interpreted as midline dimensions. The i-th stiffener plate has a thickness $t_{st,i}$, its height and width are $h_{st,i}$ and $b_{st,i}$, respectively, and now it is assumed that $h_{st,i} \leq h$ and $b_{st,i} \leq b$. The domain determined by the area of the i-th stiffener is denoted as $\Omega_{S,i}$. The transverse stiffeners are connected to the main member, in a general case, through domain $\Omega_{L,i}$. The free edges of a stiffener plate are collectively denoted as domain $\Omega_{F,i}$. The coordinate system defined in such a manner that its 'O' origin would coincide the 'C' centroid of the cross section, which is also the shear center. The member is subjected to uniform compression, by applying two end forces, assumed to be uniformly distributed over the end cross sections.

Three configurations for the connection between the member and the stiffeners are considered here. In the case of “flanges-only” connection the stiffener is connected to the flanges of the member only. In the case of “web-only” the stiffener is connected to the web of the member only. In the case of “web-and-flanges” connection the stiffener is connected to both the web and flanges of the member. The most practical case is when the stiffener is connected both to the web and the flanges, still, the other two cases have been found to be useful. It was concluded that no strong (i.e., exact) solution of the D.E. of the transverse plate can be found for the “web-and-flanges” case if the cross-section of the main member is assumed to be rigid. At the same time, if the stiffener is connected either to the web or to the flanges only, exact analytical solution for the D.E. of the transverse plate is possible. To demonstrate the validity of the newly derived formulae, thus, “flanges-only” and “web-only” cases have also been considered.

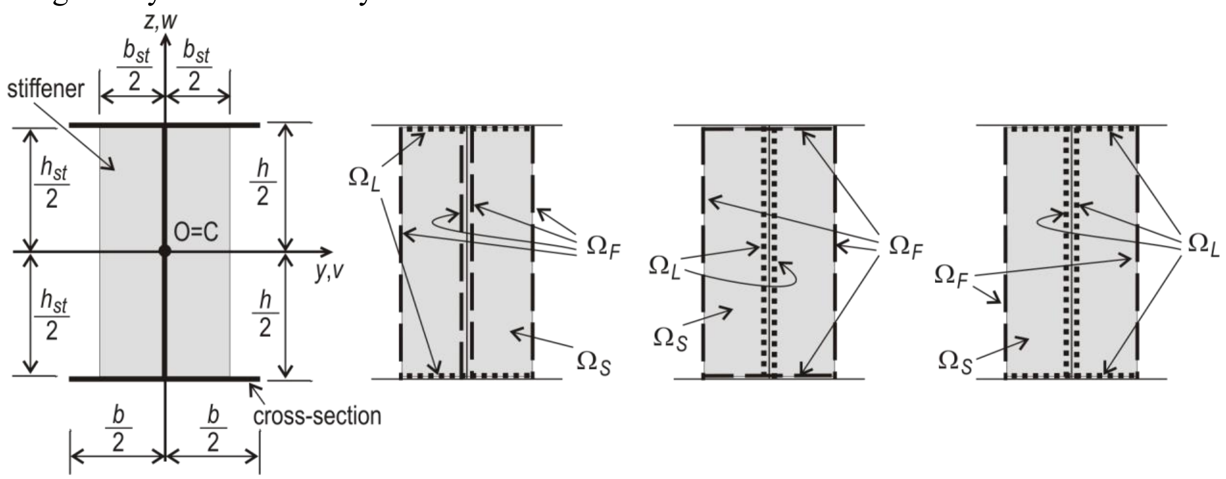

Figure 1: a) coordinates, dimensions, b) flanges-only, c) web-only, d) web-and-flanges connection

Since pure torsional buckling is investigated, the displacement of the member is described solely by the function of the twisting rotation $\theta(x)$. It has to satisfy the boundary conditions defined by the supports. It is assumed that the function is expressed as:

$$\theta(x) = \sum_1^k c_i\, f_i(x) \tag{1}$$

where c_i $(i = 1, \dots k)$ are the unknown parameters and $f_i(x)$ are predefined functions.

The u, v and w translational displacements (along the x, y and z-axis, respectively) of a general point of the member are determined as follows:

$$v_\theta(x, y, z) = \theta(x)z \tag{2}$$

$$w_\theta(x, y, z) = -\theta(x)y \tag{3}$$

$$u_\theta(\mathrm{x}, \mathrm{y}, \mathrm{z}) = \frac{\partial\theta(x)}{\partial \mathrm{x}} yz \tag{4}$$

The stiffeners are assumed to be thin plates, hence the $w_{st,i}(y, z)$ displacement function of the i-th stiffener (where $i = 1, \dots, n_{st}$) should satisfy the D.E. of the Kirchhoff-Love plate theory, plus it should satisfy the boundary conditions, too, which partly comes from the compatibility between the member and the stiffener (over domain $\Omega_{L,i}$) and partly comes from the fact that the normal stress resultant (i.e., bending moment) along the plate free edges (i.e., over domain $\Omega_{F,i}$) is zero. The D.E. of the plate is as follows:

$$\Delta\Delta w_{st,i}(y,z) = \frac{\partial^4 w_{st,i}}{\partial y^4} + 2\frac{\partial^4 w_{st,i}}{\partial y^2 \partial z^2} + \frac{\partial^4 w_{st,i}}{\partial z^4} = \frac{p_{st,i}}{D_{st,i}} \tag{5}$$

where $D_{st,i} = \frac{E t_{st,i}^3}{12(1-\nu^2)}$, is the plate stiffness and $t_{st,i}$ is thickness of the stiffener, E is modulus of elasticity, ν is Poisson's ratio, while $p_{st,i}$ is the load acting perpendicularly on the plate. In the actual column buckling problem this load is assumed to be zero, hence the right-hand-side of the D.E. is zero.

In order to derive the analytical solution for the critical load, the energy method is adopted: the total potential is expressed by some displacement parameters, then the theorem of stationarity of potential energy is used to find the equilibrium configuration. As far as the main member is concerned, the classic energy/work terms are applied. This means that the methodology followed here leads to the classic critical force formula for pure torsional buckling if no transverse stiffeners are added. However, the effect of the stiffeners is also considered. This effect is two-fold. The direct effect is that, since the stiffener plates are connected to the main member, the stiffeners will displace/deform as soon as the main member is displaced/deformed; due to this deformation strain energy is accumulated in the stiffeners that energy is to be included in the potential energy function. However, there is a second effect, too: the stiffeners modify the longitudinal displacement function of the main member.

2.2 Analysis of the stiffeners

Let us start with the case when the stiffener is connected to the flanges of the member only. Under twisting of the member, the attached stiffener is deformed. The $w_{st,i}$ displacement function of a stiffener plate should satisfy the differential equation of the plate, see Eq. (5), plus the boundary conditions, which are defined differently for each type of stiffener-to-member connection. The compatibility conditions in this "flanges-only" case are as follows.

At $z = \frac{h_{st,i}}{2}$

$$w_{st,i} = \theta'_{si}\,\frac{h_{st,i}}{2}y, \frac{\partial w_{st,i}}{\partial z} = -\theta'_{si}y \tag{6}$$

where: θ'_{si} is the first derivative of twisting function with respect to x, at the position $x = x_{st,i}$.

At $z = -\frac{hst_i}{2}$

$$w_{st,i} = -\theta'_{si}{}'\frac{h_{st,i}}{2}y, \frac{\partial w_{st,i}}{\partial z} = -\theta'_{si}y \tag{7}$$

The boundary condition for the free edges, i.e. at $y = \pm\frac{b_{st,i}}{2}$, are as follows:

$$\frac{\partial^2 w_{st,i}}{\partial^2 y} = 0 \tag{8}$$

The D.E. (5) and the above boundary conditions can be solved analytically, resulting in the following displacement function:

$$w_{st,i}(y,z) = \theta'_{si}yz - \theta'_{si}2y\left(\frac{2}{h_{st,i}^2}z^3 - \frac{z}{2}\right) \tag{9}$$

For the case when the stiffener is connected to the web of the member only, the displacement function can also be found analytically. Without showing the details, the displacement function is as follows:

$$w_{st,i} = c_i w_{st,i1} + (1 - c_i) w_{st,i2} \tag{10}$$

where:

$$w_{st,i1} = \theta'_{si} yz, w_{st,i2} = \theta'_{si} \left(y - \frac{3}{b_{st,i}} y^2 + \frac{2}{b_{st,i}{}^2} y^3 \right) z \tag{11}$$

c_i is a scalar parameter,

$$c_i = \frac{4G b_{st,i}{}^2 + 5E h_{st,i}{}^2}{24G b_{st,i}{}^2 + 5E h_{st,i}{}^2} \tag{12}$$

For the case when the stiffener is connected both to the flanges and to the web, it can be proved that no analytical solution exists, since the boundary and compatibility conditions define a singularity point. However, approximate solution is certainly possible. Here the approximate function is assumed as a perturbed version of that of the "flanges-only" case, as follows:

$$w_{st,i}(y,z) = \theta'_{si} yz - \theta'_{si} 2y \left(\frac{2}{h_{st,i}{}^2} z^3 - \frac{z}{2} \right) + f_i(y) \theta'_{si} 2 \left(\frac{2}{h_{st,i}{}^2} z^3 - \frac{z}{2} \right) \tag{13}$$

where $f_i(y)$ function (i) should be zero at $y = 0$, (ii) should have a unit first derivative at $y = 0$, and (iii) should take non-zero values only around $y = 0$, while should take zero values otherwise. These conditions are satisfied by the following function:

$$f_i(y) = \begin{cases} y - \frac{2}{\bar{b}_{st,i}} y^2 + \frac{1}{\bar{b}_{st,i}{}^2} y^3 & if \quad y \le \bar{b}_{st,i} \\ 0 & otherwise \end{cases} \tag{14}$$

where $\bar{b}_{st,i}$ is a parameter that should somehow be assumed or approximated. (According to the experiences from the numerical examples, $\bar{b}_{st,i}$ can be assumed as $0.15 b_{st,i}$ for the investigated problems).

The described $w_{st,i}$ displacement functions are illustrated in Fig. 2. The deformation in the flanges-only and web-and-flanges cases are very similar, but not identical: there is some localized waviness in the vicinity of the web in the latter case.

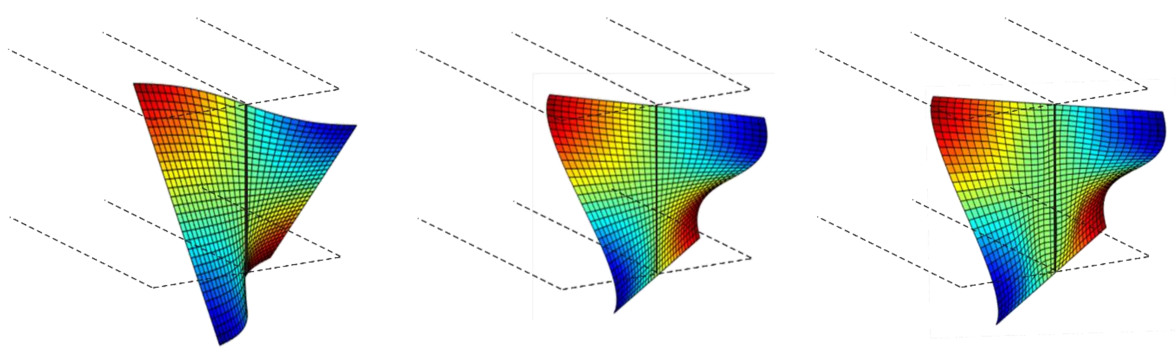

web-only flanges-only web-and-flanges

Figure 2: Stiffener deformations illustration

2.3 Critical load for clamped-clamped support case

In this Section the solution for a member with clamped-clamped supports and with n_{st} identical stiffeners is presented. Each stiffener is placed at position $x = x_{st,i}$ $(i = 1, \dots, n_{st,} 0 \leq x_{st,i} \leq L)$. For this case, the assumed longitudinal twisting displacement function is:

$$\theta = \theta_0 \frac{1}{2}\left[1 - \cos\left(\frac{2\pi x}{L}\right)\right] \tag{15}$$

This function is the well-known solution for the linear buckling of clamped-clamped members without stiffeners. Although with the presence of stiffener(s) this longitudinal twisting displacement function can be affected, it is also applicable if the stiffeners are relatively weak and regularly positioned (as we will see later).

The external potential is the negative of the work done by the loading on the (second-order) displacements. Since the only assumed loading is axial, we need the longitudinal second-order displacement only, which can be calculated from the second-order strains (i.e., relevant terms of the Green-Lagrange strain vector). The applied second-order strain, therefore:

$$\varepsilon_x^{II} = \frac{1}{2}\left(\left(\frac{\partial v_\theta}{\partial x}\right)^2 + \left(\frac{\partial w_\theta}{\partial x}\right)^2\right) = \frac{1}{2}\left(\frac{\partial \theta}{\partial x}\right)^2 (z^2 + y^2) \tag{16}$$

The external potential:

$$\Pi_{ext} = \iint \frac{F}{A} \varepsilon_x^{II} dx dA = -\frac{F r_0{}^2}{2} \int_0^L \left(\frac{\partial \theta}{\partial x}\right)^2 dx == -F r_0{}^2 \frac{\pi^2}{4L}\left(\theta_0{}^2\right) \tag{17}$$

where $r_0{}^2 = \int \frac{(z^2+y^2)}{A} \mathrm{d}A$ is the polar radius of gyration of the cross-section, F is external axial force acting on the member, and A is the cross section area.

The internal potential is the accumulated strain energy. The strain energy in the main member is due to Saint-Venant shear strains/stresses, and due to strains/stresses from warping. For the Saint-Venant strains/stresses:

$$\Pi_{int}^{S-V} = \frac{1}{2}\int_0^L G I_t \left(\frac{\partial \theta}{\partial x}\right)^2 dx = G I_t \frac{\pi}{12L}\left(3\pi \theta_0{}^2\right) \tag{18}$$

where: G is the shear modulus, I_t is the torsional constant. For the warping strains/stresses:

$$\Pi_{int}^{warp} = \frac{1}{2}\int_0^L E I_\omega \left(\frac{\partial^2 \theta}{\partial x^2}\right)^2 dx = E I_\omega \frac{\pi^3}{12L^3}\left(12\pi \theta_0{}^2\right) \tag{19}$$

where: E is the modulus of elasticity, I_ω is the warping constant.

The strain energy in a stiffener plate can be calculated from the curvatures and stress resultants (i.e., moments), as follows.

$$\Pi_{int,i}^{st} = \int_{\Omega_{S,i}} \frac{1}{2}\left(M_{st,i,yy}\kappa_{st,i,yy} + M_{st,i,yz}\kappa_{st,i,yz} + M_{st,i,zz}\kappa_{st,i,zz}\right) dy\, dz \tag{20}$$

with:

$$\kappa_{st,i,yy} = -\frac{\partial^2 w_{st,i}}{\partial y^2}, \kappa_{st,i,zz} = -\frac{\partial^2 w_{st,i}}{\partial z^2}, \kappa_{st,i,yz} = -2\frac{\partial^2 w_{st,i}}{\partial y \partial z} \tag{21}$$

and the stress resultants are as follows:

$$M_{st,i,yy} = D_{st,i}\left(\kappa_{st,i,yy} + \nu_i \kappa_{st,i,zz}\right)$$
$$M_{st,i,zz} = D_{st,i}\left(\kappa_{st,i,zz} + \nu_i \kappa_{st,i,yy}\right) \quad (22)$$
$$M_{st,i,yz} = D_{st,i}(1-\nu_i)\kappa_{st,i,yz}$$

where $D_{st,i}$ is the plate stiffness, given by Eq. (5), and ν_i is the Poisson's ratio for the *i*-th stiffener. At $x = x_{st,i}$, the strain energy in a stiffener plate is expressed by substituting the displacement function $w_{st,i}$ into Eqs. (20-22). Different stiffener-to-member connection results in different strain energy, however, it can be written with a general equation as follow:

$$\Pi_{int,i}^{st} = \frac{\pi^2}{L^2}(\theta_0)^2 \, sin^2\left(\frac{2\pi}{L}x_{st,i}\right) D_{st,i}C_{st,i} \quad (23)$$

with:

$$C_{st,i} = \frac{b_{st,i}\left(10b_{st,i}{}^2 - 9h_{st,i}{}^2\nu + 9h_{st,i}{}^2\right)}{5h_{st,i}} \quad (24)$$

$$C_{st,i} = h_{st,i}{}^2 \left[\frac{b_{st,i}}{2bst_i}(c_i - 1)^2 - \frac{b_{st,i}}{5h_{st,i}}(1-\nu)(-6c_i{}^2 + 2c_i - 1)\right], c_i \text{ see Eq. (12)} \quad (25)$$

$$C_{st,i} = \frac{b_{st,i}\left(10b_{st,i}{}^2 - 9h_{st,i}{}^2\nu + 9h_{st,i}{}^2\right)}{5hst_i} + \frac{8}{525}\frac{30\bar{b}_{st,i}{}^4 + 14\bar{b}_{st,i}{}^2 h_{st,i}{}^2 + 5h_{st,i}{}^4}{\bar{b}_{st,i}h_{st,i}}, \quad (26)$$

for "flanges-only", "web-only", and "web-and-flanges" cases, respectively.

To obtain the accumulated strain energy, we need to summarize the above energy terms:

$$\Pi_{int} = \Pi_{int}^{S-V} + \Pi_{int}^{warp} + \sum_1^{n_{st}} \Pi_{int,i}^{st} \quad (27)$$

The total potential function of the whole member is finally:

$$\Pi = GI_t \frac{\pi}{12L} 3\pi\theta_0{}^2 + EI_\omega \frac{\pi^3}{12L^3} 12\pi\theta_0{}^2 + \frac{\pi^2}{L^2}\theta_0{}^2 D_{st,i}C_{st,i}\sum_1^{n_{st}} \sin^2\left(\frac{2\pi}{L}x_{st,i}\right) - Fr_0{}^2\frac{\pi^2}{4L}\theta_0{}^2 \quad (28)$$

The minimum of the potential energy leads to a simple linear equation for *F* as follows:

$$\frac{\partial \Pi}{\partial \theta_0} = GI_t \frac{\pi}{2L}\pi\theta_0 + EI_\omega \frac{\pi^3}{L^3} 2\pi\theta_0 + D_{st,i}C_{st,i}\frac{\pi^2}{L^2} 2\theta_0 \sum_1^{n_{st}} sin^2\left(\frac{2\pi}{L}x_{st,i}\right) - Fr_0{}^2\frac{\pi^2}{2L}\theta_0 = 0 \quad (29)$$

From Eq. (29) the critical force can be expressed as follows:

$$F = \frac{1}{r_0{}^2}\left(GI_t + 4EI_\omega \frac{\pi^2}{L^2} + \frac{4}{L}D_{st}C_{st}\sum_1^{n_{st}} \sin^2\left(\frac{2\pi}{L}x_{st,i}\right)\right) \quad (30)$$

Eq. (30) indicates that there is an additional term in the critical force formula due to the presence of the stiffeners. The effect of the stiffeners is reflected in and only in this third term. This additional term can be interpreted as a weighted sum, since the stiffeners are identical, the $\sin^2\left(\frac{2\pi}{L}x_{st,i}\right)$ terms are the weights. They are related to the first derivative of the twist function, since $\sum_1^{n_{st}} \sin^2\left(\frac{2\pi}{L}x_{st,i}\right) = \frac{L^2}{\pi^2}\frac{1}{\theta_0}\sum_1^{n_{st}}(\theta'_{si})^2$. Thus, the larger the value of the first derivative of the twisting rotation function, the more effective the stiffener against torsion. It is also to highlight that (a) the Saint-Venant torsional term is independent of the length, (b) the warping term is inversely proportional to L^2, and (c) the term due to the stiffeners is inversely proportional to L. Thus, the effect of stiffeners cannot properly be represented by neither a modified I_t, nor a modified I_ω.

2.4 Critical load for pinned-pinned member with end-plates

In this Section the solution for a member with pinned-pinned supports d with two end-plates is summarized. Thus, there are two stiffeners, at $x_1 = 0$ and $x_2 = L$ and for sake of simplicity the two end-plates are identical. The solution will demonstrate the effect of the stiffeners on the twisting displacement function of the whole member. If the end-plates are very thin then the behavior of the column will approximate a classic Euler column, and if the end-plates are very thick then the behavior of the member will be similar to that of a clamped-clamped column. In the first case the displacement function (for the first buckling mode) would be a half sine-wave, while on the second case the displacement function would be a cosine function, just as in Eq. (15). It can be assumed that, with the presence of end-plates, the twisting displacement function is a linear combination of these two functions, as follows:

$$\theta = \theta_{0,1}\, sin\left(\frac{\pi x}{L}\right) + \theta_{0,2}\frac{1}{2}\left[1 - cos\left(\frac{2\pi x}{L}\right)\right] \tag{31}$$

The calculation process, presented in the previous case, must be repeated. Without showing the details of the derivations, the total potential energy function is expressed by two displacement parameters $\theta_{0,1}$ and $\theta_{0,2}$, as follows:

$$\Pi = GI_t\frac{\pi}{12L}\left(3\pi{\theta_{0,1}}^2 + 16\theta_{0,1}\theta_{0,2} + 3\pi{\theta_{0,2}}^2\right) + EI_\omega\frac{\pi^3}{12L^3}\left(3\pi{\theta_{0,1}}^2 + 16\theta_{0,1}\theta_{0,2} + 12\pi{\theta_{0,2}}^2\right) + \\ +2\frac{\pi^2}{L^2}{\theta_{0,1}}^2 D_{st}C_{st} - F{r_0}^2\frac{\pi}{12L}\left(3\pi{\theta_{0,1}}^2 + 16\theta_{0,1}\theta_{0,2} + 3\pi{\theta_{0,2}}^2\right) \tag{32}$$

In equilibrium the total potential is stationary, which leads to the following equation:

$$\begin{bmatrix} 3\pi\left(GI_t + EI_\omega\frac{\pi^2}{L^2} + \frac{8D_{st}C_{st}}{L} - F{r_0}^2\right) & 8\left(GI_t + EI_\omega\frac{\pi^2}{L^2} - F{r_0}^2\right) \\ 8\left(GI_t + EI_\omega\frac{\pi^2}{L^2} - F{r_0}^2\right) & 3\pi\left(GI_t + 4EI_\omega\frac{\pi^2}{L^2} - F{r_0}^2\right) \end{bmatrix}\begin{bmatrix}\theta_{0,1}\\ \theta_{0,2}\end{bmatrix} = \begin{bmatrix}0\\0\end{bmatrix} \tag{33}$$

The above equation can also be written as:

$$\begin{bmatrix} 3\pi(F_1 - F) & 8(F_{12} - F) \\ 8(F_{12} - F) & 3\pi(F_2 - F)\end{bmatrix}\begin{bmatrix}\theta_{0,1}\\ \theta_{0,2}\end{bmatrix} = \begin{bmatrix}0\\0\end{bmatrix} \tag{34}$$

where F_1 is the critical force that belongs to a displacement function $\theta_1 = \theta_{0,1}\sin\left(\frac{\pi x}{L}\right)$, and F_2 is the critical force that belongs to a displacement function $\theta_2 = \theta_{0,2}\frac{1}{2}\left[1 - \cos\left(\frac{2\pi x}{L}\right)\right]$. In this specific example F_{12} is equal to the critical force of a pinned-pinned column without stiffeners. The coefficient matrix of Eq. (34) must be singular, which leads to a quadratic equation as follows:

$$F^2(9\pi^2 - 64) - F(9\pi^2F_1 + 9\pi^2F_2 - 128F_{12}) + 9\pi^2F_1F_2 - 64{F_{12}}^2 = 0 \tag{35}$$

From Eq. (35) F can be calculated. It can be proved that Eq. (35) has two positive solutions. From practical point of view the smaller value is the most critical one. This critical value is dependent on the rigidity of the end-plates, hence the buckled shape of the main member is also dependent on the rigidity of the end-plates.

3. The constrained finite element method with extension for transverse plates

The constrained finite element method (cFEM) is essentially a shell finite element method, but with an ability to perform modal decomposition, see e.g. Ádány (2018), and Ádány et al. (2018). Separation of the different modes is controlled by mechanical criteria. If these criteria are enforced, the model is said to be *constrained*. Depending on the criteria the member can be constrained into e.g., global distortional, local, etc. deformation modes. The criteria can be expressed by using so-called constraint matrices which are denoted, in general, by **R**. The application of the constraint matrix enforces a certain relationship among various nodal degrees of freedom, specific to the given 'M' deformation space. This essentially means a reduction of the effective degrees of freedom. Mathematically, the **d** displacement vector is expressed as follows:

$$\boldsymbol{d} = \boldsymbol{R_M d_M} \tag{36}$$

where $\mathbf{R_M}$ is a so-called constraint matrix to the 'M' space, and $\mathbf{d_M}$ is the reduced displacement vector. Since the $\mathbf{d_M}$ reduced displacement vector has fewer elements than the original **d** vector.

If the member is supplemented by transverse plates, cFEM can still be used, see Trung and Ádány (2019). Two domains can be distinguished, depending on whether the element is part of the main member (domain 'm') or the stiffener (domain 's'), see Fig. 3. Similarly, the nodes can be separated, by assigning all the nodes of the main member to the 'm' group, while the remaining nodes to the 's' group.

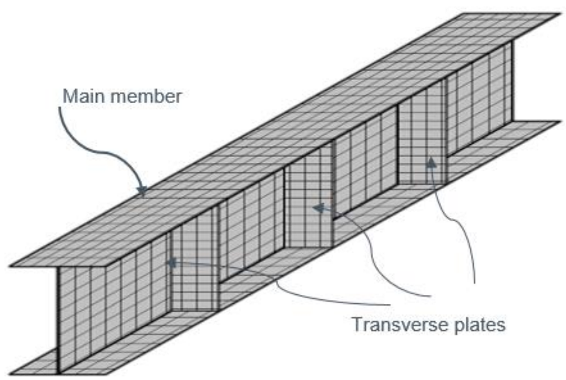

Figure 3: Thin-walled member with transverse plates

The key idea here is that the constraining should be done on the nodes in the 'm' domain by following the classic cFEM approach. However, if the main member deforms, the transverse plate elements are deformed accordingly. This deformation can be calculated by using DOF condensation. Since the column vectors of $\mathbf{R_M}$ are the modal displacement vectors of the main member, the compatible modal displacement vectors of the 's' nodes ($\mathbf{R_S}$) must satisfy the following equation:

$$\begin{bmatrix} \boldsymbol{K_{e,mm}} & \boldsymbol{K_{e,ms}} \\ \boldsymbol{K_{e,sm}} & \boldsymbol{K_{e,ss}} \end{bmatrix} \begin{bmatrix} \boldsymbol{R_M} \\ \boldsymbol{R_S} \end{bmatrix} = \begin{bmatrix} \boldsymbol{f_m} \\ \boldsymbol{f_s} \end{bmatrix} \tag{37}$$

From the second equation of Eq. (37) $\mathbf{R_S}$ can be expressed (formally) as:

$$\boldsymbol{R_S} = (\boldsymbol{K_{e,ss}})^{-1}(\boldsymbol{f_s} - \boldsymbol{K_{e,sm} R_M}) \tag{38}$$

However, additional nodal displacements in the 's' domain can be allowed, too. In this case Eq. (36) can be extended as follows:

$$\begin{bmatrix} \boldsymbol{d_m} \\ \boldsymbol{d_s} \end{bmatrix} = \begin{bmatrix} \boldsymbol{R_M} & \boldsymbol{0} \\ \boldsymbol{R_S} & \boldsymbol{I} \end{bmatrix} \begin{bmatrix} \boldsymbol{d_M} \\ \boldsymbol{\bar{d}_s} \end{bmatrix} \tag{39}$$

where $\mathbf{d_m}$ is the nodal displacement vector for the 'm' domain, $\mathbf{d_s}$ is the nodal displacement vector for the 's' domain, $\mathbf{d_M}$ and $\mathbf{R_M}$ are the same arrays as in Eq. (36), $\mathbf{I}$ is an identity matrix, and $\mathbf{R_S}$ is expressed by Eq. (38). It must be underlined here that $\bar{\mathbf{d}}_\mathbf{s}$ is that part of the displacement in the 's' domain which is not derived from the displacements of the main member. The total displacement in the 's' domain is therefore the sum of two parts: $\mathbf{R_S}\mathbf{d_M}$ comes from the displacement of the main member, and $\bar{\mathbf{d}}_\mathbf{s}$ is the displacement which is independent of the main member deformation.

4. Numerical examples

In this Section three numerical examples on the torsional buckling of I-section members are presented. The critical buckling loads are calculated using the analytical formulae presented in Section 2. Then the results are compared to cFEM solutions and also to shell finite element solution using the commercial Ansys software.

4.1 Example #1: one single stiffener

In this example a clamped-clamped I-section column member is considered with one single stiffener. The cross-section is similar to an HEA300 hot-rolled steel profile. More specifically the cross-section depth is h=300 mm, the width is b=300 mm, the flange thickness is t_f=20.5 mm, the web thickness is t_w=11.5 mm. (The depth and width values are interpreted for the midline of the cross-section.) The material is isotropic linearly elastic steel, with E=210000 MPa and ν=0.3. The stiffener width and height is equal to the width and depth of the cross-section. The t_{st} stiffener thickness varies between $0.5t_w$ and $5t_w$. Its material is identical to that of the main member. The position of the stiffener varies along the length. Two concentric axial compressive forces are applied at the member ends, equal in magnitude but opposite in direction. The forces are placed onto the member as distributed loads uniformly distributed over the cross-section.

In the Ansys model SHELL63 elements are adopted, since this element is based on the Kirchhoff-Love thin plate theory, similarly to the presented analytical solution as well as to cFEM. The sizes of the shell elements were kept approx. 50 mm for both the cFEM and the Ansys model. The clamped-clamped supports are realized so that they only prevent rotations and transverse translations, but the longitudinal translations at the supports are left free.

There is a well-known phenomenon in cFEM: critical loads calculated to global buckling by constrained buckling analysis are bigger than the analytical results. This is due to the restrained transverse deformations, as explained in detail in Ádány and Visy (2012). A possible way to eliminate this effect is to set the Poisson's ratio to zero. Thus, ν=0.0 is used here for the main member. However, ν=0.3 is applied for the stiffener.

In Table 1 the presented results belong to L=8 m, stiffener position x_s=2000 mm, and t_{st} is either t_w or $2t_w$. The results are shown for the three types of stiffener-to-member connection. The cFEM results show practically precise agreement with the analytical results in all the cases, the difference being less than 1%. The analysis results clearly show the importance of the stiffener-to-member connection. The connection to the flanges is much more efficient than the connection to the web. The "web-and-flanges" type connection leads to the largest critical load values, though these critical load values are only 10% larger than those in the "flanges-only" case, i.e., the connection to the flanges seem to be responsible for about 90% of the increasing of the critical load due to the stiffeners. Based on this observation, and considering that the analytical solution for the "web-and-flanges" type is approximate, in all the following examples the "flanges-only" connection type will be used.

Table 2 illustrates the effect of the stiffener position on the critical load. Results are shown for two t_{st} values. The values in the table are the critical stress increments (in N/mm^2) caused by the stiffener, with respect to the critical stresses without the stiffener (1064.1 N/mm^2, 1051.9 N/mm^2, and 1065.6 N/mm^2 from the analytical, Ansys, and cFEM calculations, respectively, see Table 1). It can be observed that the tendencies of the results from all the analyses are the same, in the case of the thinner stiffener even the numerical values are fairly similar. According to the analytical solution, see Eq (30), the effect of the stiffener position is included only in the sinusoidal term, so the increments in any row of Table 2 should be proportional to the corresponding $(\sin)^2$ values as follows:

$$\sin^2\left(\frac{\pi}{4}\right) = \frac{1}{2} \ : \ \sin^2\left(\frac{2\pi}{4}\right) = 1 \ : \ \sin^2\left(\frac{3\pi}{4}\right) = \frac{1}{2} \ : \ \sin^2\left(\frac{4\pi}{4}\right) = 0$$

Indeed, the increments in Table 2 follow precisely this pattern in the case of the analytical and the cFEM calculations, and almost precisely in the case of the shell FEM calculation, too.

Table 1: Critical stresses[1] with one stiffener, L=8 m, x_s=2 m

		no stiffener	web-only	flanges-only	web-and-flanges
$t_{st} = t_w$	analytical	1064.3	1065.5	1075.2	1076.3
$t_{st} = t_w$	Ansys	1051.9	1052.5	1060.3	1060.7
$t_{st} = t_w$	cFEM	1065.6	1066.7	1076.4	1077.3
$t_{st} = 2t_w$	analytical	1064.3	1073.3	1151.2	1160.0
$t_{st} = 2t_w$	Ansys	1051.9	1055.3	1093.4	1093.8
$t_{st} = 2t_w$	cFEM	1065.6	1074.1	1144.8	1150.7

Table 2: Critical stress increment[2] due to one stiffener, L=8 m, flanges-only connection

		1000mm	2000mm	3000mm	4000mm
$t_{st} = t_w$	analytical	5.4	10.9	5.4	0.0
$t_{st} = t_w$	Ansys	4.2	8.4	4.2	0.0
$t_{st} = t_w$	cFEM	5.3	10.8	5.4	0.0
$t_{st} = 2t_w$	analytical	43.4	86.8	43.4	0.0
$t_{st} = 2t_w$	Ansys	21.1	42.7	21.2	0.5
$t_{st} = 2t_w$	cFEM	37.0	79.2	37.7	0.0

In Table 3 the effect of the member length on the critical load is illustrated. The analyzed members have one stiffener at $x=0.25L$, and $t_{st}=t_w$. The considered lengths are large enough, which is necessary to avoid the influence of local deformations in the Ansys-FEM results. If the increment critical loads are plotted with respect to the member length, the result is a hyperbolic curve, see Fig. 4 (left); and if a doubly logarithmic scale is applied, the curve is a straight line with 45 deg

[1] Critical stresses unit is [N/mm^2].
[2] Critical stresses increment unit is [N/mm^2].

inclination, see Fig. 4 (right). This observation is fully supported by the analytical solution, given by Eq. (30): the increment is proportional to the inverse of the member length.

Table 3: Critical stresses with one stiffener, $t_{st}=t_w$, $x_s=0.25L$, flanges-only connection

		6m	8 m	10m	12m	16m
no stiffener	analytical	1594.2	1064.3	819.1	685.9	553.4
no stiffener	Ansys	1561.3	1052.4	812.5	681.5	551.0
no stiffener	cFEM	1596.1	1065.6	820.1	686.7	554.1
with stiffener	analytical	1608.7	1075.2	827.8	693.1	558.8
with stiffener	Ansys	1573.0	1061.0	819.3	687.2	555.4
with stiffener	cFEM	1610.4	1076.4	828.7	693.9	559.4

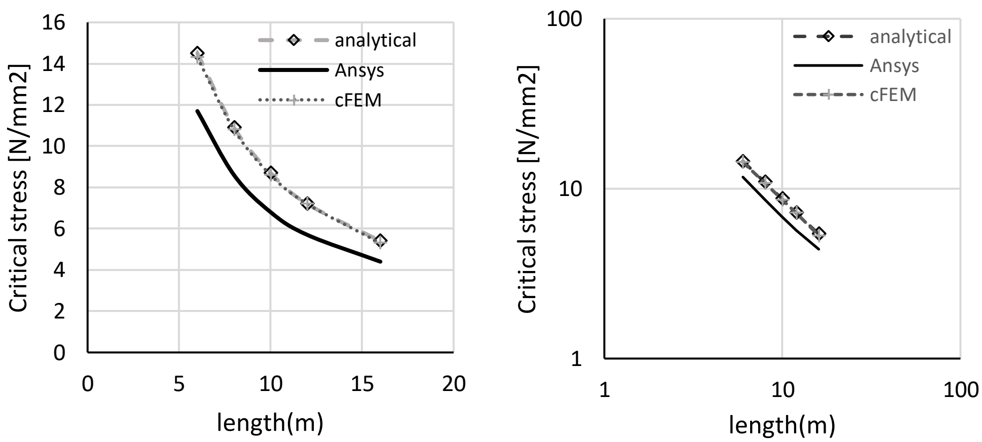

Figure 4: Critical stress increments due to one stiffener, $t_{st}=t_w$, $x_s=0.25L$, flanges-only connection

In all the above cases the cFEM and the analytical results are in strong agreement with each other. The Ansys results show a systematic difference, though the tendencies are the same. The slightly different numerical results from the Ansys analyses are most surely due to the fact that in both the cFEM and the analytical solution the cross-sections are truly rigid, i.e., only rigid-body cross-section displacements are allowed, while the Ansys model is unconstrained, i.e., small local flexural deformations in the plate elements, and/or transverse extensions, and/or membrane shear deformations are allowed and do occur. The very good agreement of the cFEM and analytical results seem to be universal, at least if the stiffeners are thin enough. For thicker stiffeners larger differences might exist, discussed as follows.

In Table 4 the effect of the stiffeners thickness is demonstrated. When the stiffener is relatively thin ($t_{st}/t_w \leq 2$), the cFEM results are nearly coincidental with the analytical ones. However, if the stiffener thickness is increasing, the difference between the cFEM and the analytical solutions is increasing (see e.g. $t_{st}/t_w = 5$). This observation can be explained by the fact that the twisting displacement function is fixed in the analytical solution (in this example: a cosine wave), but can be arbitrary in the cFEM. This observation also proves the general conclusion from Section 2.4: the presence of the stiffeners has an effect on the longitudinal distribution of the twisting displacement of the main member, too. As Fig. 5 shows, the tendency is clear: the stronger the stiffener, the stronger its effect on the main member's displacements.

4.2 Example #2: multiple stiffeners

In this Example #2 the problem is essentially identical to that of Example #1, but instead of one single stiffener, there are multiple stiffeners which are equally spaced along the length of the 8 m member. The analysis results are summarized in Fig. 6.

Table 4: Critical stress increments due to one stiffener, L=8 m, x_s=2 m, flanges-only connection

	t_{st}/t_w=0.5	t_{st}/t_w=1	t_{st}/t_w=1.5	t_{st}/t_w=2	t_{st}/t_w=5
analytical	1.357	10.85	36.63	86.82	1357
Ansys	0.958	8.447	23.06	41.53	244.3
cFEM	1.362	10.78	35.28	79.21	434.1

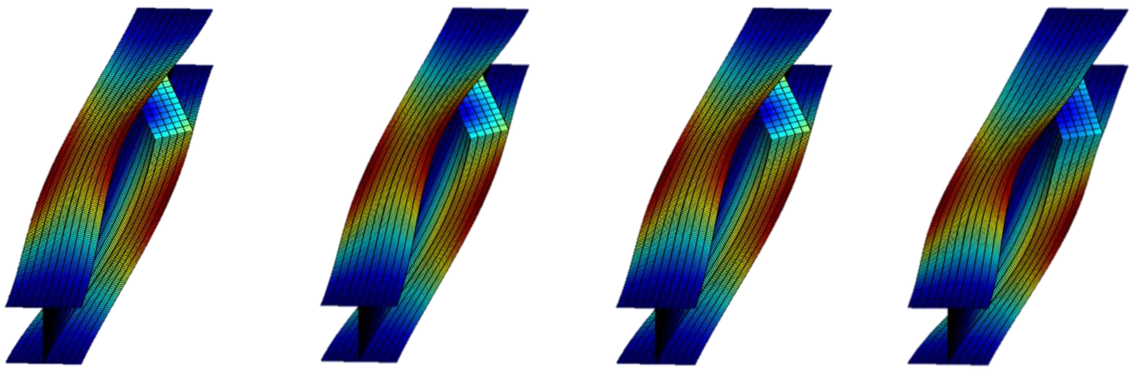

t_{st}/t_w=0.5 t_{st}/t_w=1 t_{st}/t_w=2 t_{st}/t_w=5

Figure 5: Constrained torsional buckling displacement shapes, L=8 m,

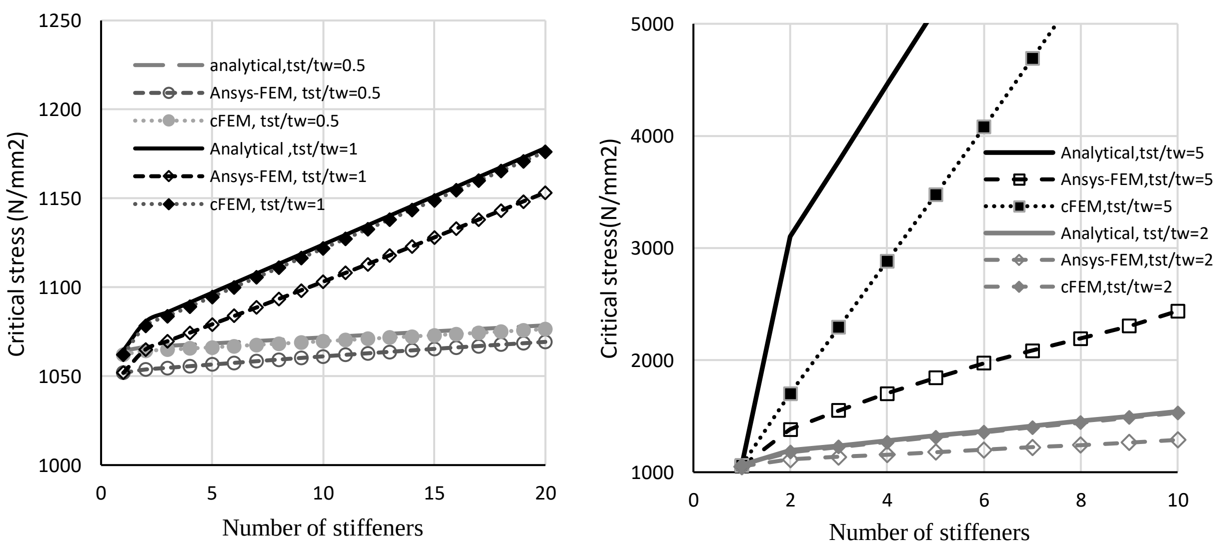

Figure 6: Critical stresses in the function of the number of stiffeners, L=8 m

The critical load (or load increment) is linearly changing with the number of stiffeners, which can be proved mathematically by the analytical formulae. The linearly increasing tendency is clearly observable from the Ansys-FEM results and cFEM results, too. (It is to note that in certain cases it is not possible to find a pure torsional mode in the Ansys-FEM solution, due to the large number of buckling modes with lower critical load values. This is the situation, for example, with the 8-m-long column having more than 10 stiffeners with t_{st}=5t_w.) The plots also demonstrate what has already been observed in the previous example: with relatively thin stiffener, the cFEM and analytical results are nearly coincident, however, the thicker the stiffeners are, the larger the difference is between the predictions from the various methods. In the case of ordinary FEM it can be observed that thick stiffeners generate waviness in the flanges (see Fig. 7), which means that the torsional buckling is coupled with some local buckling; that explains the significant difference between ordinary FEM and the other methods. In the case of cFEM the local deformations are eliminated by the constraining, still, the buckled shape from cFEM can be different from that of the analytical assumption: unlike in analytical solution, there is no certain pre-defined twisting displacement function in cFEM, which explains the differences between the cFEM and the analytical critical load values.

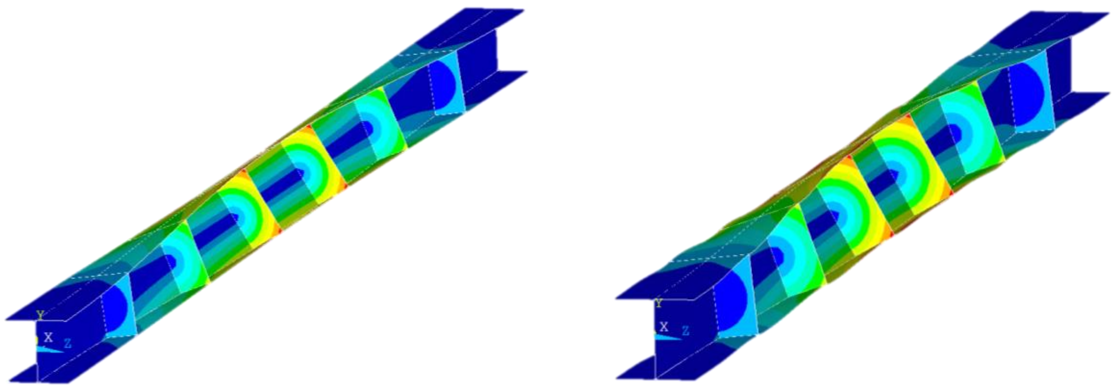

t_{st}/t_w=0.5 t_{st}/t_w=5

Figure 7: Buckling shapes, L=8 m, 6 stiffeners

4.3 Example #3: pinned-pinned member, two end-plates

In this Example #3 the problem is similar to that of Example #1: the cross-section and material are the same, but now the end supports are pinned and there are end-plates at both member ends (and no further stiffeners). Two different member lengths are analyzed, while the t_{st}/t_w ratio varies from 0.5 to 20. The results are summarized in Fig. 8. In the plot the critical stresses are presented (for two member lengths) in the function of the end-plate thickness. The first observation is that the critical load is bounded, and the boundary is dependent on the member length. Indeed, the explanation of this observation is presented in Section 2, where the twisting displacement function (see Eq. (31)) for the analytical derivation is introduced. When the end-plates are very thin, the member behaves as a member without end-plates; the twisting function is a half sine-wave. The extremely thick end-plate works as a clamped support; the twisting function is a cosine function (as in Eq (15)). Between the 'very thin' and 'extremely thick' situations there is a gradual change of the twisting function, which is visible by the buckled shapes, see Fig. 9. The analysis clearly shows a discrepancy between the Ansys results and the results from the other two methods; the discrepancy is caused by the various non-global deformations in the Ansys solution. At the same time, it is remarkable that, despite the end-plate thickness range is extremely wide, the cFEM and the analytical solutions are practically identical for both member length. This means that the assumed twisting function (Eq. 31) in Section 2.4 correctly captures the pure torsional buckling behavior, hence the analytical solution of Eq. (35) can be applied for a wide range of members with end-plates.

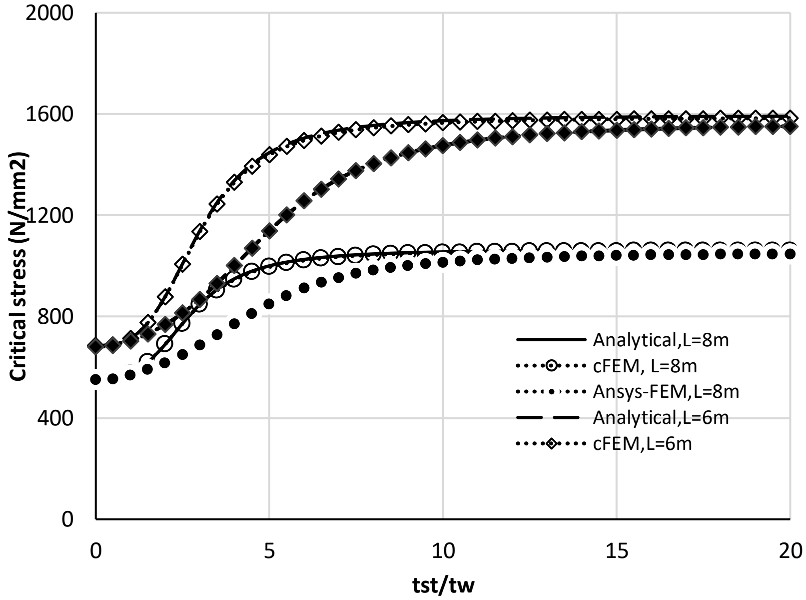

Figure 8: Critical stresses, pinned member with two end-plates, cFEM, Ansys FEM and analytical solutions

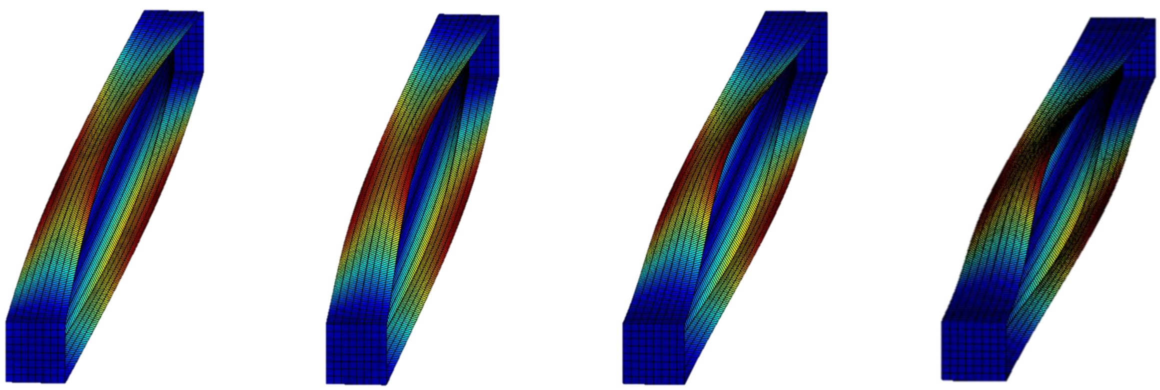

t_{st}/t_w=0.5 t_{st}/t_w=2 t_{st}/t_w=4 t_{st}/t_w=10

Figure 9: cFEM buckling displacement shapes, L=8 m, flanges-only connection

5. Summary

In this paper the effect of transverse plate elements (referred also simply as "stiffeners") on the torsional buckling of the doubly symmetrical I section columns is discussed. Closed-form analytical solutions are derived for the critical force by using the energy method. Several numerical examples are presented in which the analytical results are compared to the results from shell finite element linear buckling analyses. The shell finite element results are obtained by the commercial Ansys software, as well as by the specific constrained finite element method (cFEM) in which the cross-section deformations have been eliminated. The comparison shows practically the same tendencies in all the three methods. Particularly, the cFEM and the analytical results are coincident if the stiffeners are weak. In the case of stronger stiffeners the analytical solution may overestimate the critical force. The critical loads by an ordinary shell FE analysis are typically lower due to the always existing local deformations, which make it practically impossible to precisely calculate pure global buckling.

The analytical formulae as well as the numerical results show that the transverse plate elements have two major effects on the buckling of the member. The *direct* effect is due to the deformation of the stiffeners. The second, *indirect* effect is that the introduction of stiffeners can (and typically do) modify the longitudinal distribution of the twisting rotations of the member which results in changing of the critical force.

The *direct* effect is always associated with the increment of the critical load, which can be characterized as follows: (a) it is linearly proportional to the inverse of the length of the member, (b) it is proportional to the plate stiffness (of the stiffener), that is highly sensitive to the thickness of the stiffener, (c) it is dependent on the stiffener geometry, and strongly influenced by the stiffener-to-member connection, and (d) it is also influenced by the position of the stiffener along the length of the member, the efficiency being proportional to the value of the first derivative of the twisting rotation function of the main member. The *indirect* effect is primarily dependent on the ratio between the stiffness of the member and the stiffness of the stiffeners, but also influenced by many other factors, such as the arrangement of the stiffeners, etc.

The presented analytical solutions help to better understand the effect of transverse elements on the torsional behavior of thin-walled members. The formulae can further be generalized in certain extent, e.g., to analyze lateral-torsional buckling of beams with transverse plate elements. However, arbitrary cases seem to be too complicated to be handled by analytical solutions. For these cases numerical solutions can be used, most notably the constrained finite element method, the applicability of which has been proved by the here presented examples.

Acknowledgement

The presented work was conducted with the financial support of the K119440 project of the National Research, Development and Innovation Office of Hungary.

References

Ádány S. (2018), Constrained shell Finite Element Method for thin-walled members, Part 1: constraints for a single band of finite elements, Thin-Walled Structures, Vol 128, July 2018, pp. 43-55.

Ádány S., Visy D., Nagy R. (2018), Constrained shell Finite Element Method, Part 2: application to linear buckling analysis of thin-walled members, Thin-Walled Structures, Vol 128, July 2018, pp. 56-70.

Ádány S., Visy D. (2012), Global Buckling of Thin-Walled Columns: Numerical Studies, *Thin-Walled Structures*, 2012, Vol 54, pp 82-93.

Ansys, Release 19.2, 2019.

Chroscielewski J., Lubowiecka I., Szymczak C., Witkowski W. (2006), On some aspects of torsional buckling of thin-walled I-beam columns, *Computers & Structures*, Vol 84, Issues 29–30, 2006, pp. 1946-1957.

Fujii K., Ohmura H. (1985), A Study of Rigidity and Strength in Torsion of H-Beam Stiffened with Transverse Stiffeners, *Proc. OF JSCE Structural Eng./Earthquake Eng.*, Vol 2, No. 1, April 1985, pp. 289-292.

Hoang T., Ádány S. (2019), Modal analysis of thin-walled members with transverse plate elements using the constrained finite element method, *Proceedings* of the International Colloquium on Stability and Ductility of Steel Structures (SDSS 2019), Prague, Czech Republic 11-13 September 2019, pp. 499-507.

Rao C.K., Rao L.B. (2017), Torsional post-buckling of thin-walled open section clamped beam supported on Winkler–Pasternak foundation, *Thin-Walled Structures*, 116, 2017, pp. 320-325.

Taras A., Greiner R. (2008), Torsional and flexural torsional buckling - A study on laterally restrained I-sections, *Journal of Constructional Steel Research*, Vol 64, Issues 7–8, July–August 2008, pp. 725-731.

Vlasov V.Z. (1961), Thin-walled Elastic Beams, National Science Foundation, Washington, DC, 1961.